Note: This is a draft of a paper being submitted for publication. Contents of this paper should not be quoted nor referred to without permission of the authors.

CONF-790653--2

EQUILIBRIUM PROPERTIES OF THE FLUXOID LATTICE IN SINGLE-CRYSTAL NIOBIUM

H. R. Kerchner
D. K. Christen
S. T. Sekula
P. Thorel

SOLID STATE DIVISION
OAK RIDGE NATIONAL LABORATORY
Operated by
UNION CARBIDE CORPORATION
for
U. S. DEPARTMENT OF ENERGY

June 1979

EQUILIBRIUM PROPERTIES OF THE FLUXOID LATTICE IN SINGLE-CRYSTAL NIOBIUM[1]

H. R. Kerchner
D. K. Christen
S. T. Sekula
P. Thorel[2]

Solid State Division
Oak Ridge National Laboratory
Oak Ridge, Tennessee

I. INTRODUCTION

The dimensions and symmetry of the fluxoid lattice in a single-crystal sphere of niobium have been measured by using a double-perfect-crystal small-angle neutron-scattering technique (DCSANS). The bulk magnetization of the same sample has been measured by a field-sweep technique. In addition, the misalignment between the fluxoids and the applied magnetic field was observed by DCSANS. The experimental methods and most of the results are reported elsewhere (Kerchner *et al.*, 1979; Christen *et al.*, 1979). Here we summarize our findings and compare the measurements with realistic microscopic theory where it is available.

The DCSANS technique gives directly the symmetry, orientation, and dimensions of the fluxoid-lattice unit cell. The flux density per unit cell, deduced by using the flux quantization condition, is plotted in Fig. 1. In the intermediate mixed state (IMS) of the sphere the flux density per unit cell is independent of the applied field H_a while the bulk flux

[1]*Research sponsored by the Division of Materials Science, U. S. Department of Energy, under contract W-7405-eng-26 with the Union Carbide Corporation.*
[2]*Guest Scientist from Départemente de la Recherche Fondementale, Centre d'Etudes Nucléaires, Grenoble, France.*

density (solid curve) rises linearly with H_a. In the mixed state (MS) the sample is filled with fluxoid lattice and the two quantities are identical.

The fluxoid lattice observed was hexagonal only when the applied field was parallel to a <111> crystal direction. Usually the lattice was constructed of isosceles triangles whose orientation sometimes reflected the symmetry of the crystal. At some orientations the crystal symmetry was reflected only in the random occurrence of two different, symmetrically disposed fluxoid lattices. For fields in a <100> direction, we observed a structural phase transition near 2 K between a square lattice and a scalene-triangle lattice.

The field-sweep technique gives directly the field derivative of the magnetization, dM/dH_a. The magnetization $M(H_a)$ was obtained by numerical integration. The Meissner state, the IMS, the MS, and the normal state show up as distinct regions of the $M(H_a)$ and dM/dH_a plots shown in Fig. 2. Since the Meissner state usually superheats and the magnetization is hysteretic in the IMS, only MS data were used to determine the equilibrium properties.

Detailed comparisons between our magnetization measurements and various results of Gorkov theory are described elsewhere (Kerchner *et al.*, 1979; Christen *et al.*, 1979). We have little new to add to the well-known discrepancies between Gorkov theory and the magnetization of niobium. Some recent theoretical effort has been made to relate the relative anisotropy of the lower and upper critical fields H_{c1} and H_{c2} and the limiting value of dM/dH_a at H_{c2} to the anisotropy of the Fermi surface. In addition, the effects of a strong, retarded electron-phonon interaction on H_{c2} and the thermodynamic critical field H_c have recently been investigated theoretically. Those theoretical results are compared with our data below. Since our measurements of the anisotropy of H_{c2} are substantially identical to earlier results (Seidl *et al.*, 1978), they will not be discussed here.

II. ANISOTROPY RESULTS

In Fig. 3 are plotted detailed measurements of the orientation dependence of the lower critical field H_{c1} and the equilibrium flux density B_o at H_{c1}. The anisotropy of H_{c1} was measured by three independent techniques. The circles in Fig. 3 were derived from DCSANS measurements of B_o and the field $H_2 = \frac{2}{3} H_{c1} + \frac{1}{3} B_o$ bounding the IMS and the MS. The solid curve in the upper part of the figure was found by fitting a cubic harmonic expansion of the thermodynamic expression (Christen *et al.*, 1979; Takanaka and Nagashima, 1979),

$$H_a \Delta\psi = -\frac{2}{3}\, dH_{c1}/d\alpha, \qquad (1)$$

to the measured misalignment angle $\Delta\psi$ between $\vec{B}_o$ and $\vec{H}_a$ in the IMS. Here α is the angle between $\vec{H}_a$ and the [001] direction in a symmetry plane of the crystal. The bulk magnetization was measured at many temperatures for fields in the three high-symmetry directions, and the deduced values of H_{c1}/H_c were fitted to an expansion in cubic harmonics and in powers of $(1 - T/T_c)$. The temperature dependences of the cubic harmonic coefficients deduced are shown in Fig. 4, and the corresponding values of $H_{c1}/\bar{H}_{c1}$ at 4.3 K for the three high-symmetry directions are shown in Fig. 3. The agreement among the three measurements demonstrates the reliability of our determination of the anisotropy of H_{c1}. The anisotropy of B_o could be resolved only by DCSANS measurements of the fluxoid lattice in the IMS.

The limiting temperature dependence of $\Delta H_{c1}/H_{c1}$ near T_c has been related to the Fermi surface average,

$$\langle v_x^4\rangle/\langle v^4\rangle - .2 \simeq .058\ [2\langle v^2 H_4(\hat{v})\rangle/\langle v^2\rangle - \langle H_4(\hat{v})\rangle] \qquad (2)$$

(Takanaka and Hubert, 1975), where v_x is the projection on [001] of the Fermi velocity $\vec{v}$ and $H_4(\hat{v})$ is the $\ell = 4$ cubic harmonic evaluated in the direction of $\vec{v}$. The right-hand side of Eq. (2) has been calculated by using band-theory (Butler, 1979) and has been deduced from the measured anisotropy of H_{c2} (Seidl *et al.*, 1978). The two values are in good agreement, and the predicted anisotropy of H_{c1} agrees well with the observations as shown in Fig. 4.

The limiting value of dM/dH_a at H_{c2} was read off the field-sweep plots and the parameter κ_2 deduced by using the definition,

$$4\pi[dM/dH_a]_{H_{c2}} = [\beta(2\kappa_2{}^2 - 1) + \tfrac{1}{3}]^{-1}. \qquad (3)$$

The experimental values of κ_2 were fitted as for the H_{c1}/H_c data. The best-fit temperature dependences of the cubic harmonic coefficients are plotted in Fig. 5. The limiting temperature dependence of $\Delta\kappa_2/\kappa$ depends on the parameter

$$\langle v_x^4 - .2v^4\rangle/\langle v^2\rangle^2 \simeq .058[2\langle v^2 H_4(\hat{v})\rangle/\langle v^2\rangle - \langle H_4(\hat{v})\rangle] \qquad (4)$$

(Berthel and Pietrass, 1978). Again, the theoretical result agrees well with the observations.

III. H_c RESULTS

The temperature dependence of H_c is sensitive to the strength of the electron-phonon interaction in strong-coupling superconductors. Our measurements are compared with recent theoretical calculations (Daams and Carbotte, 1978) based on two different tunneling-derived phonon spectra in the deviation-function plot of Fig. 6. The MIT spectrum ($\lambda = .33$) is too weak. The Stanford spectrum ($\lambda = .98$) is slightly too strong. Daams and Carbotte adjusted the Stanford spectrum ($\lambda = .89$) to make the deviation function fall close to earlier calorimetric determinations. This latter curve falls on our measurements at low temperatures but below them near T_c. Using functional derivatives evaluated for the Stanford spectrum by Daams and Carbotte, we have determined that adding weight to the phonon spectrum at high energy (subject to the constraint of constant T_c) raises the high-temperature portion of the predicted deviation function as indicated by the vertical arrow without appreciably affecting the low-temperature portion.

Our H_c measurements indicate that the electron-phonon enhancement parameter $\lambda \approx .91$. This result is too small to account for the experimental enhancement of the band velocity deduced by Crabtree *et al.* (1979). The mean-square (renormalized) Fermi velocity of Crabtree *et al.* gives nearly the observed H_{c2} near T_c (Hohenberg and Werthamer, 1967) when the strong-coupling enhancement (Rainer and Bergmann, 1974) is taken into account. Thus the discrepancy is clearly a theoretical problem, probably due either to incorrect band velocities or to the neglect of a significant electron-electron component of the many-body-theory mass enhancement.

IV. CONCLUSIONS

To conclude, we want to emphasize that in favorable cases mixed-state measurements on type-II superconductors can be made very precisely. A number of features of the mixed state are sensitive to the microscopic electronic structure of the material; therefore, they are not described accurately by Gorkov theory, and they can serve as sensitive tests of realistic microscopic theory. The theoretical connection between the mixed state and microscopic material properties is difficult and correspondingly incomplete, but where the connection exists it works well, as demonstrated by our results.

ACKNOWLEDGMENTS

The authors are grateful to H. Harmon and Y. K. Chang for preparing the samples. W. H. Butler and J. P. Carbotte explained much of the microscopic theory to us and supplied results of their theoretical calculations before publication.

REFERENCES

Berthel, K.-H, and Pietrass, B. (1978). *J. Low Temp. Phys. 33*, 127.
Butler, W. H. (1979). Private communication and this volume.
Christen, D. K., Kerchner, H. R., Sekula, S. T., and Thorel, P. (1979).
Crabtree, G. W., Dye, D. H., Karim, D. P., Koelling, D. D., and Ketterson, J. B. (1979). *Phys. Rev. Letters 42*, 390.
Daams, J. M., and Carbotte, J. P. (1978). *In* "Inst. Phys. Conf. Ser. No. 39," p. 715.
Hohenberg, P. C., and Werthamer, N. R. (1967). *Phys. Rev. 153*, 493.
Kerchner, H. R., Christen, D. K., and Sekula, S. T. (1979).

Rainer, D., and Bergmann, G. (1974). *J. Low Temp. Phys. 14*, 501.
Seidl, E., Weber, H. W., and Teichler, H. (1978). *J. Low Temp. Phys. 30*, 273.
Takanaka, K., and Hubert, A. (1975). *In* "Proceedings of the Fourteenth International Conference on Low Temperature Physics" (M. Krusius and M. Vuorio, ed.), p. 309. American Elsevier, New York.
Takanaka, K., and Nagashima, T. (1979). To be published in J. Phys. Soc. Jap.

FIGURE 1. The bulk flux density (solid curve) vs applied field H_a, compared to the average flux density/unit cell obtained from DCSANS. The inset shows how the flux density/unit cell is found from the flux quantum condition.

FIGURE 2. Experimentally measured dM/dH_a and $M(H_a)$ obtained by numerical integration.

FIGURE 3. Experimental data at T = 4.30 K for the anisotropy of the low-field critical parameters B_o and H_{c1} for applied fields in the (1$\bar{1}$0) and (100) niobium crystal planes.

FIGURE 4. Temperature dependences of the cubic harmonic coefficients for H_{c1}.

FIGURE 5. Temperature dependences of the cubic harmonic coefficients for κ_2.

FIGURE 6. The deviation function for the temperature dependence of the thermodynamic critical field H_c. The solid curves represent calculations based on tunneling-derived phonon spectra.

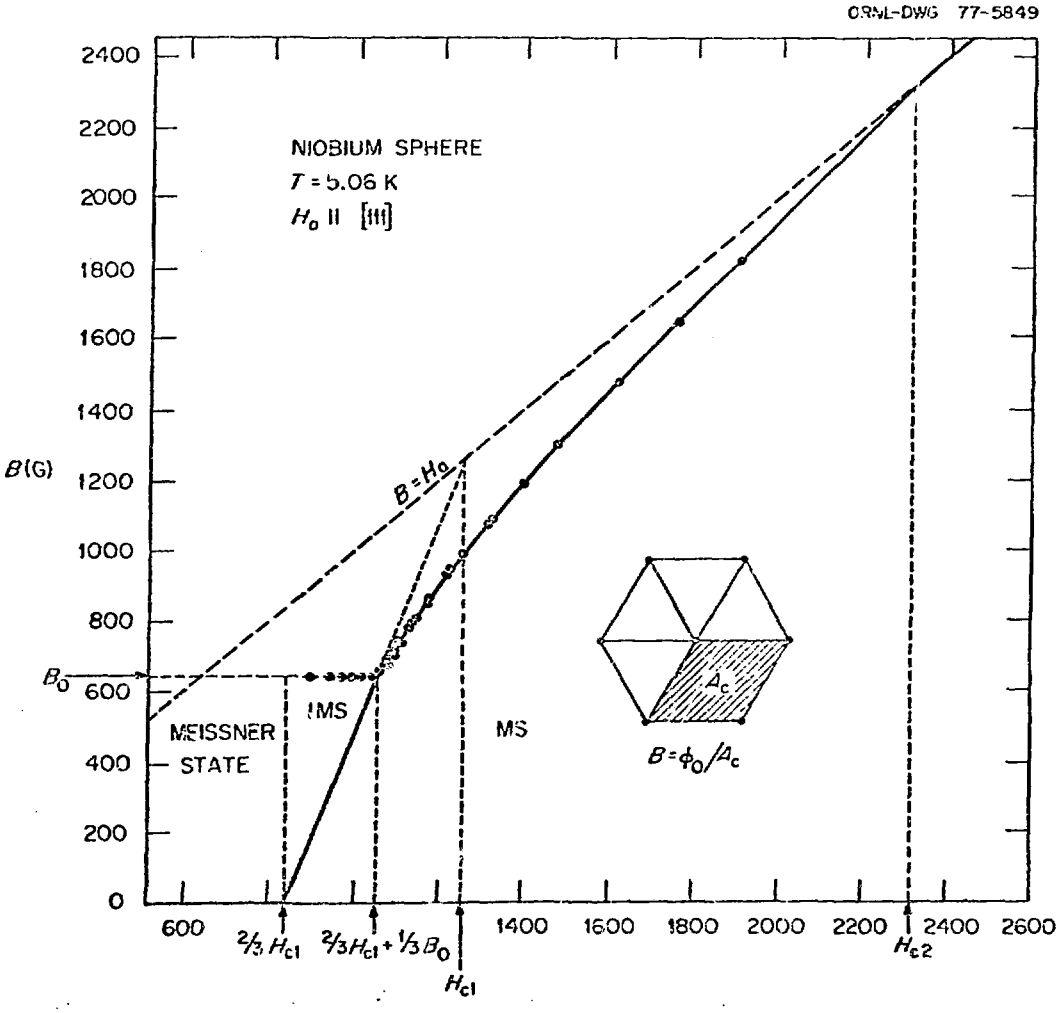
ORNL-DWG 77-5849
NIOBIUM SPHERE
T = 5.06 K
H0 II [111]
B(G)
B = H0
B0
MEISSNER STATE
IMS
MS
MS
Δc
B = φ0/Δc
2400
2200
2000
1800
1600
1400
1200
1000
800
600
400
200
0
600
2/3 Hc1
2/3 Hc1 + 1/3 B0
Hc1
1400
1600
1800
2000
2200
2400
2600
Hc2

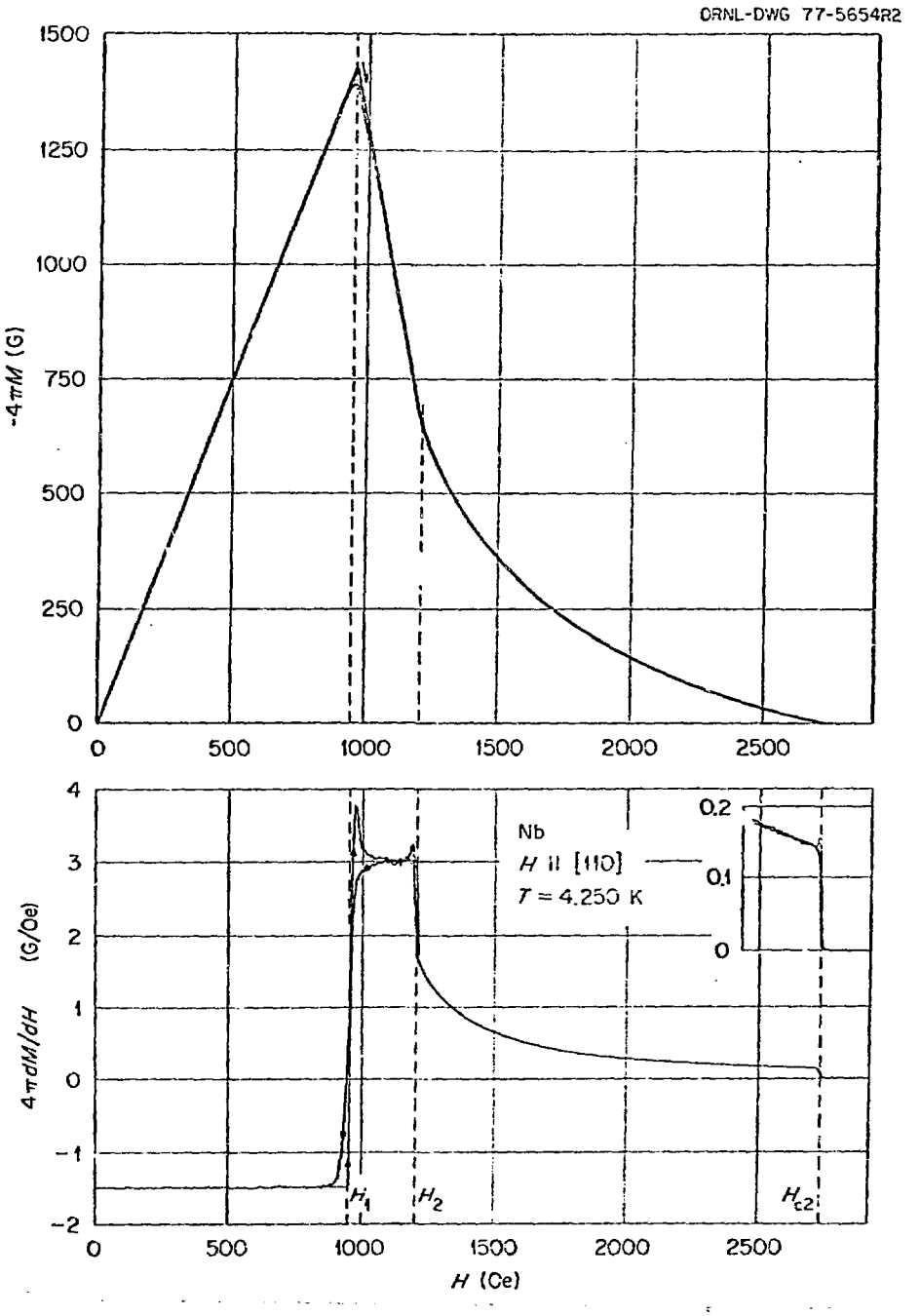
ORNL-DWG 77-5654R2
1500
1250
1000
750
500
250
0
-4πM (G)
0
500
1000
1500
2000
2500
4
3
2
1
0
−1
−2
4πdM/dH (G/Oe)
Nb
H ll [110]
T = 4.250 K
0.2
0.1
0
H1
H2
Hc2
H (Oe)

ORNL-DWG 78-18353

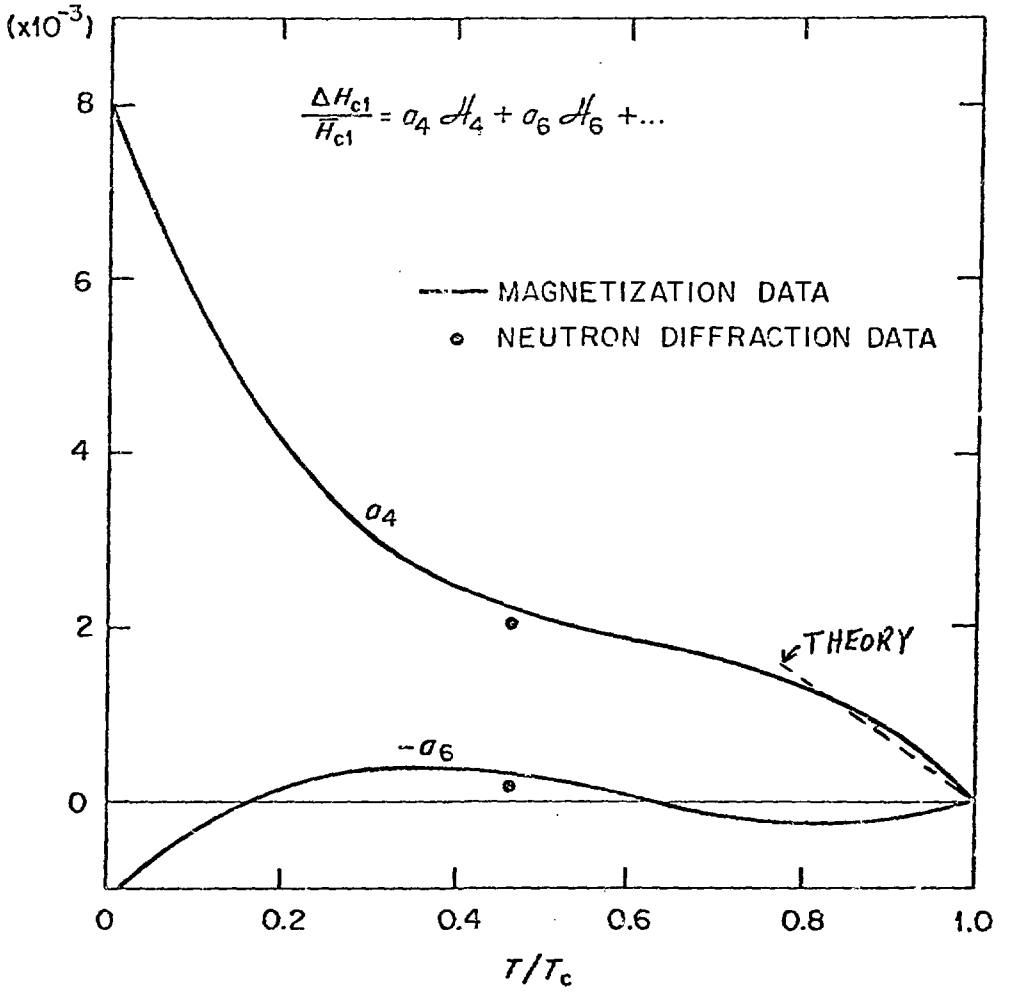

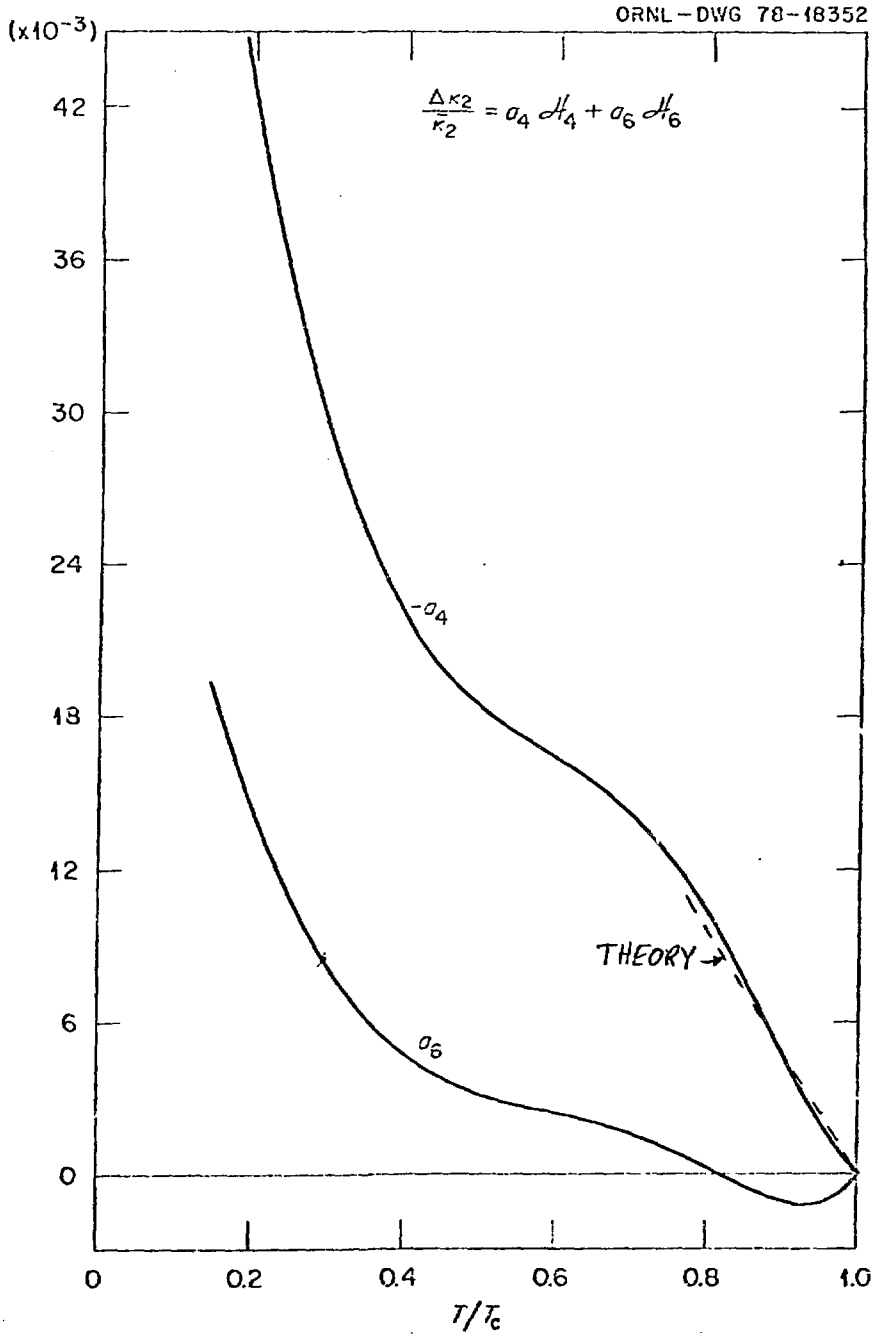
ORNL-DWG 78-18352
(x10⁻³)
42
36
30
24
18
12
6
0
$\frac{\Delta\kappa_2}{\kappa_2} = a_4 \mathcal{H}_4 + a_6 \mathcal{H}_6$
$-a_4$
a_6
THEORY
0
0.2
0.4
0.6
0.8
1.0
T/T_c

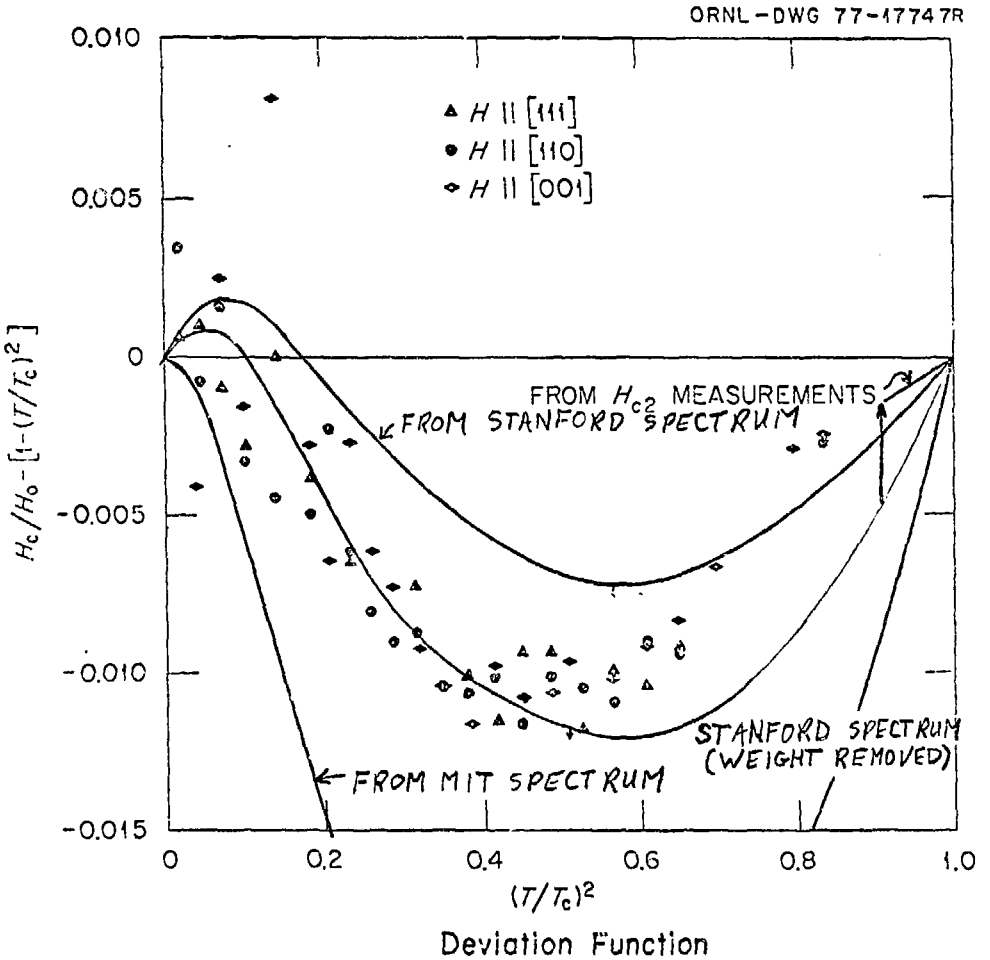

Deviation Function